

## Deliverable D4.3

# Candidate materials for couplings and casings

Grant agreement no.	654497		
Duration	01.02.2016 – 31.01.2019		
Work package	WP4 – Flexible coupling and casing materials		
Type	R - document, report		
Dissemination level	PU - public		
Due date	31.07.2016		
Actual submission data	12.07.2016		
Lead author	I.Thorbjornsson		
Contributors			
Version	1.0		
Document status			
Change history	Version	Date	Changes



This publication was completed with the support of the European Commission and European Union funding under Horizon 2020 research and innovation programme. The contents of this publication do not necessarily reflect the Commission's own position. The document reflects only the author's views and the European Union and its institutions are not liable for any use that may be made of the information contained here.



## Executive summary

Selection of materials for high temperature geothermal wells follow Oil and Gas (O&G) standards and recommendations and the same apply for wellhead design, well design and drilling. Geothermal wells differ from O&G wells with higher temperatures and non-condensable gases such as H<sub>2</sub>S and CO<sub>2</sub> and often low pH level. These are all parameters which have corrosive effect on the well material and often more complicated forms of corrosion than in common O&G wells. It is therefore of high importance for long life of geothermal wells to select casing materials that can both withstand the high temperature and the corrosive nature of the geothermal fluid. The goal of this report is to describe the corrosive nature of geothermal environment and reveal the material research performed and validate the findings according to high temperature/pressure use in geothermal wells. This literature study has further the goal to present a research plan for filling the gaps in testing, if any, and especially to look into possible use of material combination such as cladding of high alloyed (high cost) corrosion resistant materials on lower alloyed (lower cost) material. The cladded corrosion resistant material is in direct contact with the steam/brine but is only a thin layer on the base material of commonly used carbon steel which in turn is protected from the steam by the thin corrosion resistant layer. This material combination is ideal to optimize the corrosion resistance with respect to cost. Also an important issue for this is to prevent galvanic corrosion to occur between the high alloyed layer and the base material and to avoid damaging effect of different thermal expansion coefficients for the thin layer and the base material.



## Contents

<b>1</b>	<b>Introduction.....</b>	<b>7</b>
<b>2</b>	<b>Corrosion in geothermal wells.....</b>	<b>7</b>
2.1	Material testing in geothermal environment.....	10
2.2	Uniform corrosion .....	12
2.3	Pitting corrosion.....	15
2.4	Hydrogen affected corrosion.....	16
2.5	Stress corrosion cracking.....	18
2.6	Galvanic corrosion.....	21
<b>3</b>	<b>Materials for geothermal wells.....</b>	<b>23</b>
3.1	Carbon steels .....	23
3.2	Stainless steels.....	24
3.3	Nickel alloys.....	26
3.4	Titanium.....	26
<b>4</b>	<b>Conclusions .....</b>	<b>27</b>
<b>5</b>	<b>References .....</b>	<b>29</b>

## Tables

Table 2.1.	<i>Gas composition for three high temperature geothermal fields in Iceland. ..</i>	9
Table 2.1.1.	<i>Chemical composition and physicochemical parameters of the IDDP-1 steam.....</i>	11
Table 2.1.2.	<i>Nominal chemical composition of the materials selected for testing in the IDDP-1 steam. ....</i>	12

## Figures

Figure 2.1.	<i>Schematic layout of well KJ 39. ....</i>	8
Figure 2.2.	<i>Pictures showing severe corrosion of well liner in the Krafla geothermal field well KJ-39.....</i>	8
Figure 2.3.	<i>S-N curves for 12% Cr turbine steel in three geothermal sites and in air. The effect of hydrogen is evident in Reykjanes results.....</i>	9
Figure 2.1.1.	<i>Picture taken of the material test rank for testing in the IDDP-1 well in the Krafla area in NE Iceland.).....</i>	10
Figure 2.1.2.	<i>Pictures taken of the material test rank inside the pipe leading to the silencer of the IDDP-1 well.....</i>	11
Figure 2.2.1.	<i>Material from either liner or casing in the IDDP-1 well. Retrieved during flow testing of the well (Photo from A. Einarsson). ....</i>	13
Figure 2.2.2.	<i>Retrieved part of liner from the KJ 39 well in Krafla. ....</i>	14
Figure 2.2.3.	<i>Picture showing the retrieve of the uppermost 8 meters of the IDDP-1 wellhead for inspection .....</i>	14
Figure 2.2.4.	<i>Measured corrosion rates in mm/year of the materials tested in the IDDP-1 well.....</i>	15

Figure 2.3.1. *Pitting corrosion on the inside of a pipe of stainless steel type AISI 316* 16

Figure 2.4.1. *An image from Scanning Electron Microscope (SEM) of 17-4 ph steel after corrosion fatigue testing*..... 16

Figure 2.4.2. *A tensile testing specimen after slow stain testing.* ..... 17

Figure 2.4.3. *A tensile testing specimens after slow stain testing.* ..... 17

Figure 2.5.1. *Stress corrosion cracking on the outside of a pipe from AISI 316 stainless steel* ..... 18

Figure 2.5.2. *SEM images of the cross-section of the U-bend specimens* ..... 19

Figure 2.5.3. *SEM images of the cross-section of the U-bend specimens* ..... 20

Figure 2.5.4. *SEM images of the cross-section of the U-bend specimens* ..... 21

Figure 2.6.1. *The galvanic series in sea water*..... 22

Figure 2.6.2. *Figure showing severe galvanic corrosion on one-way valve where the house is made of Cast Iron with connector and sieve made of Bronze.* ..... 22

Figure 3.1.1. *SEM images of the cross-sections of the carbon steels after testing*.... 24

Figure 3.2.1. *SEM images of the cross-sections of the stainless steels after testing*.. 25

Figure 3.3.1. *SEM images of the cross-sections of the nickel alloys after testing*..... 26

Figure 3.4.1. *SEM images of the cross-sections of the titanium alloys after testing* ... 27

## 1 Introduction

The geothermal industry, scientists and material providers have been actively looking into the corrosion nature of geothermal steam and brine for many years. This has resulted in better material selection for geothermal use, mainly in the surface equipment like valves, steam separators, pipes and not least in the turbines. More recently the focus has been moving over to the wells, traditionally designed according to O&G standards with respect to materials. In this report the focus will be on higher temperature wells, meaning temperature above 250°C. The corrosive nature of the geothermal steam/brine is highly site dependent; the corrosive aggressiveness of geothermal fluids can vary from sour wells in volcanic sites to dry wells in older geothermal systems. The effect of non-condensable gases is of high importance, especially the partial pressure of H<sub>2</sub>S that can trigger material cracking as Hydrogen Introduced Cracking (HIC) or as SSCC (Sulphide Stress Corrosion Cracking). Beside the effect of low pH and amount of gases one has to look to free halogens such as Chloride (Cl<sup>-</sup>) which can trigger corrosion pitting and general corrosion. For non-ferrous materials like Titanium, gases like Fluorine (F) are of interest as well. It is therefore clear that material selection for a given well is not a straight forward task, it has to be taken based on the site specific conditions. Today the selection is based on API (American Petroleum Institute) and NACE (National Association of Corrosion Engineers) standard and guidelines of materials, selected for Oil and Gas wells. The materials that are most common are low carbon grades and in most cases these material grades have proven to be successful. Today many wells with these materials have been in operation for over 30 years. But there are as well several examples where these materials have not been sufficient as will be shown in this report. Going into deeper and higher temperature fields generate furthermore increased interest in the materials as the more aggressive fluid in deeper geothermal sites calls for more resistant material solutions. This report will first reveal the various corrosion problems found in geothermal wells, reveal materials tested for geothermal use and in the end list candidate materials. Focus will be on thin layer of more corrosion resistant materials on base material of low cost, normally referred to as cladded material. Methods for cladding include spraying, welding, explosion cladding and directly extruded pipes. In this report corrosion test results from Icelandic high temperature (>250°C) geothermal wells will be reviewed and discussed. Most of the testing has been related to the Iceland Deep Drilling Project well 1 (IDDP-1) but other wells have as well been evaluated and are included in this report.

## 2 Corrosion in geothermal wells

Corrosion in geothermal wells has been in research focus for many years. The importance of understanding why corrosion occurs and the chemical reaction of the material surface with geothermal fluid is of high importance for long life of geothermal wells. The pH level together with geothermal gases and free halogens like Cl<sup>-</sup> are known corrosion factors. The effect of mixing zones within the well where f.ex. colder steam entering the well mixes with higher temperature steam from lower part of the well is also important as it can create local conditions which are not possible to monitor at the surface. This situation, illustrated in Figure 2.1, can result in very aggressive environment and cause rapid corrosion as can be seen in Figure 2.2. In this case, the steel used in the affected well showed high corrosion rate where the 12 mm wall thickness of the slotted liner was fully corroded with severe pitting corrosion and hydrogen embrittlement. The liner was retrieved from the well in this condition after only few weeks of service.

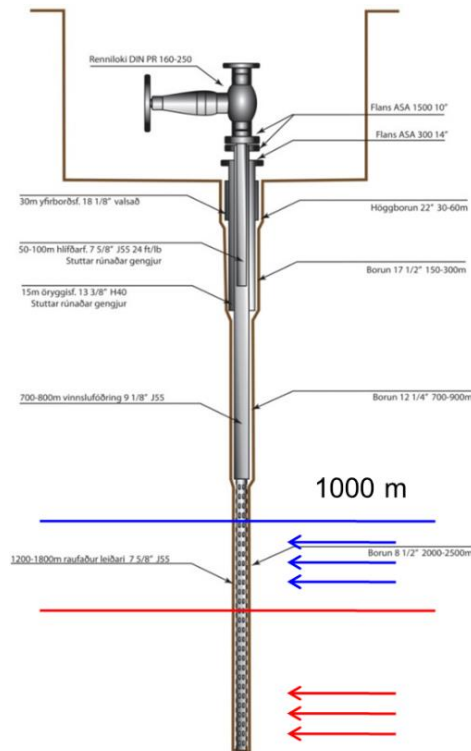


**Figure 2.1.** Schematic layout of well KJ 39.



**Figure 2.2.** Pictures showing severe corrosion of well liner in the Krafla geothermal field well KJ-39. Corrosion of well liner at a blending point between HCl containing dry steam from lower geothermal system and wet fluid from upper system.

Materials in dry steam wells have shown to be affected by Hydrogen Embrittlement, as shown later in this report, but generally the materials (K55, L80) used for the well casing and liner have shown to be long lasting. Exceptions are buckling and formation of so called bulges in the production casing resulting from stresses in the material as a result of thermal expansion during warming up of the well.

Properties of geothermal fluid vary from one field to another. The content of non-condensable gases and pH level are different and therefore the corrosion behaviour and material

performance as well. Table 2.1 (Thorbjornsson, 1995) shows the gas composition for three high temperature fields in Iceland at that time, but the nature of geothermal fields is to develop and change with time.

**Table 2.1.** Gas composition for three high temperature geothermal fields in Iceland.

	CO <sub>2</sub> (%)	H <sub>2</sub> S (%)	H <sub>2</sub> (%)	N <sub>2</sub> (%)	% of total steam
Krafla	96.5	1.5	1.5	-	1.2
Nesjavellir	39.3	25.3	33.1	2.1	0.4
Reykjanes	95.2	2.3	1.5	0.9	0.4

It has been shown that during fatigue testing in geothermal steam, this variation in gas content as well as the presence of Cl<sup>-</sup> in the Reykjanes area result in different material performance in these three fields. Figure 2.3 shows corrosion fatigue testing of turbine material of the 12% Cr type in air as well as geothermal in situ testing.

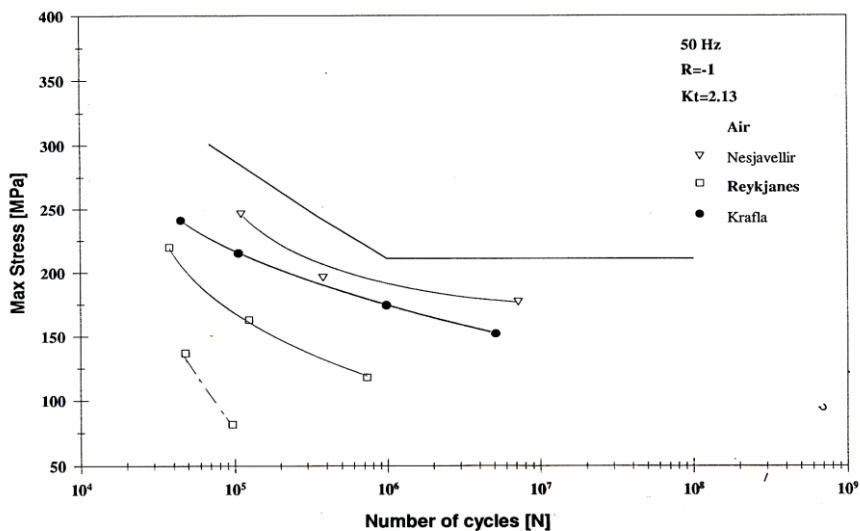


**Figure 2.3.** S-N curves for 12% Cr turbine steel in three geothermal sites and in air. The effect of hydrogen is evident in the Reykjanes results. (Thorbjornsson, 1995).

Further it can be seen in Figure 2.3. that there are actually two curves for testing in the Reykjanes area. This is believed to be due to variation in steam velocity during testing, where the curve with higher live time is where low flow rate was set to normal operation, and the other when the flow rate was higher. With increased flow rate the risk of droplets carrying Cl<sup>-</sup> ions entering the test chamber is higher. It should be noted that each data point on the graph is a mean value of at least 4 specimen tested.

The main types of corrosion detected for well materials in high temperature wells is the focus of the following sections. Understanding the corrosion behaviour and resistance will then form the knowledgebase for selecting materials that can withstand corrosion for a predicted lifetime of the well.

## 2.1 Material testing in geothermal environment

Materials used in high temperature/pressure geothermal fluid can be subjected to corrosion due to the aggressiveness of the geothermal fluid and non-condensable gases such as hydrogen sulphide (H<sub>2</sub>S) and carbon dioxide (CO<sub>2</sub>), chloride ions (Cl<sup>-</sup>) and hydrogen fluoride (HF) as described earlier in this report. The fluid composition varies from one field to another as can be seen in Table 2.1 and even between wells in the same area. Further the geothermal fields have the tendency to change in the gas content during utilization and build-up of scaling can be important for the resistance of materials to corrosion. Figure 2.1.1 shows test rack for materials to be tested in the Iceland Deep Drilling Project well (IDDP-1) in the Krafla area in NE Iceland. The IDDP-1 well was measured with well head temperature of 452°C at 140 bar pressure flowing 12 kg/s of superheated steam and thus the highest temperature measured in geothermal well worldwide.



**Figure 2.1.1.** *Picture taken of the material test rack for testing in the IDDP-1 well in the Krafla area in NE Iceland. Specimens were both stressed (u bend specimens) and unstressed, welded and not welded (Karlsdottir et al., 2015)*

Figure 2.1.2 shows how the test rack from Figure 2.1.1 is covered with scaling when inspected after some three weeks of testing. The silica scaling is totally sealing off the specimen from the steam and by that preventing corrosive elements to come into contact with the test coupons, lowering or even stopping corrosion of the materials.

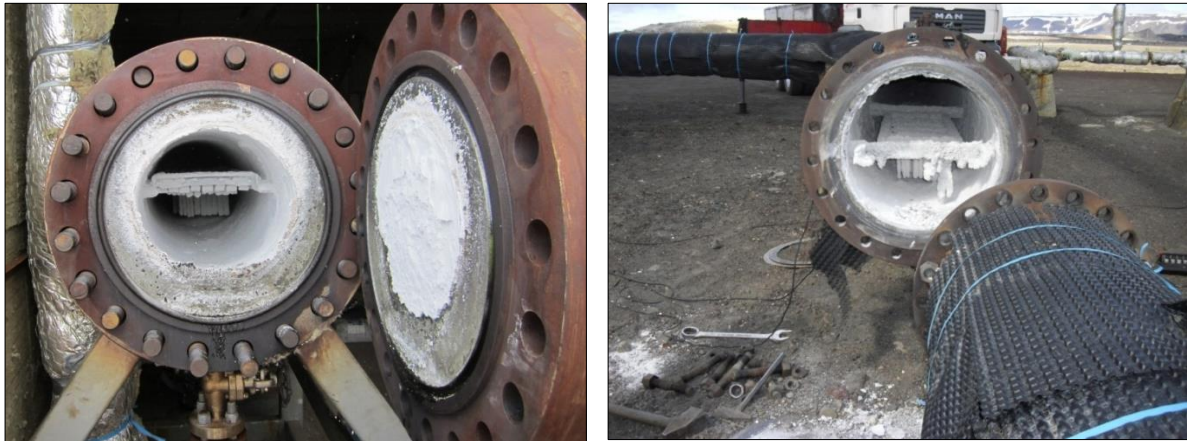


**Figure 2.1.2.** Pictures taken of the material test rank inside the pipe leading to the silencer of the IDDP-1 well. Situation after three weeks of testing revealing massive scaling inside the pipe and on the test specimens. (Karlsdottir et al., 2015).

The chemical composition of the steam in the IDDP-1 well is shown in table 2.1.1. Material selection for the testing is revealed in Table 2.1.2. The selection was based on both the existing as well as candidate materials for geothermal wells and surface pipes and equipment.

**Table 2.1.1.** Chemical composition and physicochemical parameters of the IDDP-1 steam (Hauksson et al., 2014).

pH@ 240-270°C		2.7
CO <sub>2</sub>	(mg/kg)	339
H <sub>2</sub> S	(mg/kg)	732
H <sub>2</sub>	(mg/kg)	10
Cl	(mg/kg)	93
F	(mg/kg)	5.0
Fe	(mg/kg)	8.4
B	(mg/kg)	1.0

**Table 2.1.2.** Nominal chemical composition of the materials selected for testing in the IDDP-1 steam. (Thorbjornsson et al, 2015).

Material	Grade*	Elements (wt%)																			
		C	Si	Mn	P	S	Cr	Ni	Mo	N	Cu	Co	Al	Nb	Ti	V	W	H	O	Pd	Fe
<i>Carbon steel</i>	EN 1.0425	0.2	0.4	0.8-1.4	0.025	0.015	0.3	0.3	-	0.012	0.3	-	0.02	0.02	0.03	0.02	-	-	-	-	Bal.
	API K55	0.4	0.4	1.6	0.03	0.008	-	-	-	-	-	-	-	-	-	-	-	-	-	-	Bal.
	API TN95	0.3	0.3	0.6	-	0.003	1.0	-	0.5	-	-	-	-	-	-	-	-	-	-	-	Bal.
<i>Austenitic stainless steel</i>	S30403	0.03	1.0	2.0	0.045	0.03	18.0-20.0	8.0-12.0	-	-	-	-	-	-	-	-	-	-	-	-	Bal.
	S31603	0.03	1.0	1.5	0.045	0.03	16.0-18.0	10.0-14.0	2.0-3.0	-	-	-	-	-	-	-	-	-	-	-	Bal.
	N08904	0.02	1.0	2.0	0.045	0.035	19.0-23.0	23.0-28.0	4.0-5.0	-	-	-	-	-	-	-	-	-	-	-	Bal.
	S31254	0.02	0.8	1	0.03	0.01	20.0	18.0	6.1	0.2	0.7	-	-	-	-	-	-	-	-	-	Bal.
	N08028	0.02	0.6	2.0	0.025	0.015	27.0	31.0	3.5	-	1.0	-	-	-	-	-	-	-	-	-	Bal.
<i>Duplex stainless steel</i>	S31803	0.03	1.0	2.0	0.03	0.015	22.0	5.0	3.2	0.18	-	-	-	-	-	-	-	-	-	-	Bal.
	S32750	0.03	0.8	1.2	0.035	0.015	25.0	7.0	4.0	0.3	-	-	-	-	-	-	-	-	-	-	Bal.
	S32770	0.03	0.5	1.5	0.035	0.01	27.0	6.5	4.8	0.4	-	1.0	-	-	-	-	-	-	-	-	Bal.
<i>Ni-based alloys</i>	N06255	0.03	1.0	1.0	0.03	0.03	23.0-26.0	47.0-54.0	6.0-9.0	-	1.2	-	-	-	0.69	-	3.0	-	-	-	4.0-17.0
	N08825	0.05	0.5	1.0	-	-	19.5-23.5	38.0-46.0	2.5-3.5	-	1.5	-	0.2	-	0.6-1.2	-	-	-	-	-	22.0
	N06625	0.1	0.5	0.5	-	-	20.0-23.0	60.0-64.0	8.0-10.0	-	-	1.0	0.4	-	0.4	-	-	-	-	-	5.0
<i>Non-ferrous alloys</i>	R50400	0.1	-	-	-	-	-	-	-	0.03	-	-	-	-	99.2	-	-	0.15	0.25	-	0.3
	R52400	0.1	-	-	-	-	-	-	-	0.03	-	-	-	-	99.0	-	-	0.15	0.25	0.2	0.3

\* UNS number unless other specified

## 2.2 Uniform corrosion

Uniform corrosion is the most common corrosion form for carbon and low alloy steels. This form of corrosion requires moisture or other electric conducting media on the surface where anode-cathode reaction can take place. This corrosion is measured on coupons where they are weighted before and after testing. The weight loss is related to the surface area of the coupons and often represented as corrosion rate in mm/year. General acceptance for corrosion rate in geothermal environment is not set by standards but often the acceptance limit is set to 0.1 mm/year. This form of corrosion is more often discovered on the outside of wells, especially at the wellhead where the casings exceed from the cement. This is mostly due to the fact that it is not possible to measure or detect degradation due to corrosion in well material down-hole. Therefore, the cases for detecting corrosion and measure its effect have been on material pieces that have been detected coming up with the steam as seen in Figure 2.2.1, or where the liner has been retrieved to surface after exposure in the well, see Figure 2.2.2. In some cases, the uppermost 8-10 meters have been excavated after the well was shut down permanently by removing the ground surrounding the well as can be seen in Figure 2.2.3.

General corrosion is characterised by the following anode-cathode reaction:

- Anode:  $M \rightarrow M^{n+} + ne^{-}$
- Cathode:  $O_2 + 2H_2O + 4e^{-} \rightarrow 4OH^{-}$  or  $2H^{+} + 2e^{-} \rightarrow H_2$

The oxygen reaction is the dominant cathodic reaction if  $\text{pH} > 5.5$  and there is oxygen present. Hydrogen evolution increases rapidly at  $\text{pH} \leq 5.5$  and gradually becomes the dominant reaction.

The absence of a fast cathodic reaction often limits corrosion in geothermal systems.



**Figure 2.2.1.** Material from either liner or casing in the IDDP-1 well. Retrieved during flow testing of the well (Photo from A. Einarsson).

The anodic reaction produces metal ions  $\text{M}^{n+}$ . The metal ions generally combine with other ions in the electrolyte to form a solid corrosion product on the metal surface were the most common of these is rust which consists of iron oxides and hydroxides,  $\text{Fe}(\text{OH})_3$  -  $\text{Fe}_2\text{O}_3$  (red rust) or  $\text{Fe}_3\text{O}_4$  (magnetite, black rust). In highly acid fluids little or no solid corrosion products are generally formed on the corroding metal surface as can be seen in Figure 2.2.2.



**Figure 2.2.2.** Retrieved part of liner from the KJ 39 well in Krafla. Severe damages due to uniform corrosion. No corrosion products detected.



**Figure 2.2.3.** Picture showing the retrieve of the uppermost 8 meters of the IDDP-1 wellhead for inspection (Photo from the National Power Company – Landsvirkjun).

Results from testing down-hole in well IDDP-1 are shown in Figure 2.2.4. Coupons were attached to a test rank as shown in Figure 2.1.1 and put inside pipe from the well to silencer as seen in Figure 2.1.2. As can be seen, the corrosion rate for low-medium carbon steels are much higher than for stainless steel types as expected and the higher alloyed Ni alloys are with very low values close to detection limits. Lower alloyed Ni alloy N088255 suffer from higher corrosion rate.

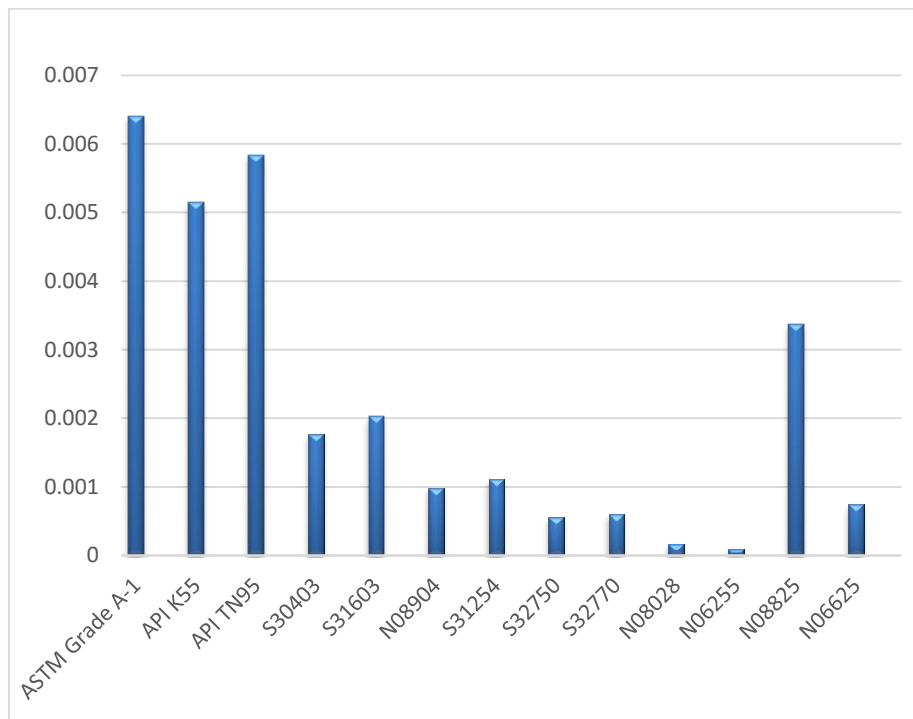


**Figure 2.2.4.** Measured corrosion rates in mm/year of the materials tested in the IDDP-1 well. (Karlsdottir et al. 2015)

### 2.3 Pitting corrosion

Pitting corrosion is highly localized corrosion forming cavities or holes in the metal surface. The starting points for pit formation in steel are often MnS inclusions or other impurities in the metal surface. For steels containing passive films such as stainless steels the local destruction of the passive film is commonly due to presence of chlorides. The resistance of pitting for steels can be calculated according to the Pitting Resistance Equivalent Number (PREN) and can be used for comparison between different types of steels, mostly stainless steels. The PREN is calculated according to standard ISO 15156-3 Materials for use in H<sub>2</sub>S containing environments and the formula is given as:

$$PREN = \%Cr + 3.3 (\%Mo + \%W) + 16 \%N$$

For common stainless steels used in the geothermal industry the PREN value is:

- SS 304                      PRE ≈ 19
- SS 316                      PRE ≈ 25
- SAF 2205                    PRE ≈ 35
- SAF 2507                    PRE ≈ 43
- SS 904L                     PRE ≈ 35
- 254 SMO                    PRE ≈ 43
- 654 SMO                    PRE ≈ 56
- Sanicro28                  PRE ≈ 39 (27% Cr, 31%Ni, 3,5%Mo, 1%Cu)



**Figure 2.3.1.** *Pitting corrosion on the inside of a pipe of stainless steel type AISI 316. (Photo Thorbjornsson).*

## 2.4 Hydrogen affected corrosion

Geothermal gases contain Hydrogen Sulphide,  $H_2S$ , but the amount varies from field to field as can be seen in Table 2.1. The gas can react with the metal surface were either  $MnS$  or  $FeS$  form and the metal sulphide prevents formation of hydrogen molecules on the surface resulting in Hydrogen ions diffusing into the steel as well as some ions escaping into molecules in the geothermal steam. The ions diffusing into the steel will either pass through the metal or stop typically at micro voids, slag inclusions or other defects. In these voids the hydrogen ions form molecules and by that multiply in volume. This will increase the pressure in the micro voids and the pressure can be so high as to form crack inside the metal. This phenomenon can clearly be seen in Figure 2.4.1 (Thorbjornsson, 1995).

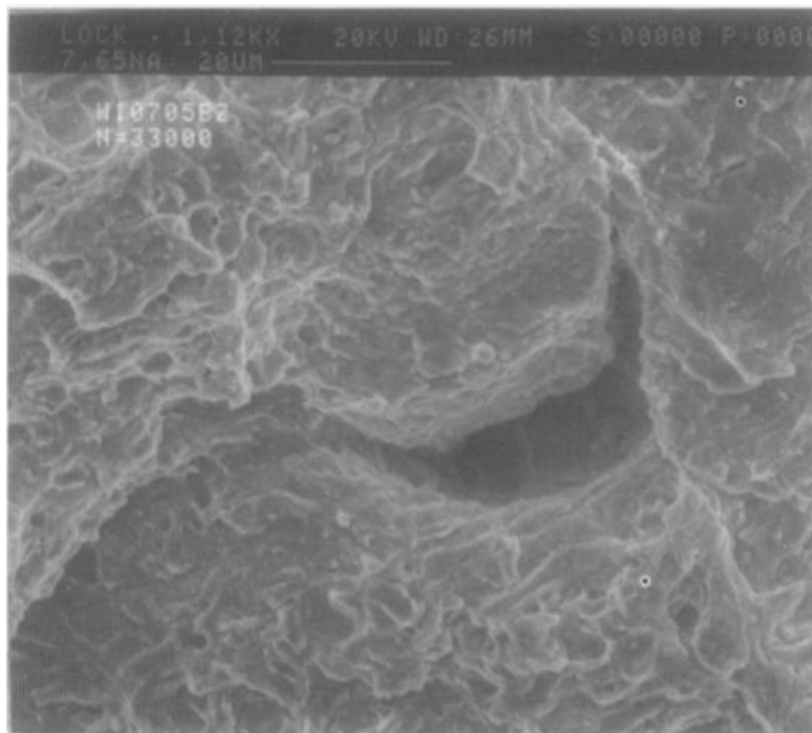


**Figure 2.4.1.** *An image from Scanning Electron Microscope (SEM) of 17-4 ph steel after corrosion fatigue testing (Thorbjornsson, 1995). Picture reveal cracking around the grain boundary due to hydrogen embrittlement.*

Slow strain testing ( $2 \times 10^{-6}$ ) of material from existing wells in Iceland (Well 8 in Reykjanes and Well 5 in Nesjavellir) (Thorbjornsson 1994) revealed that although the material has no sign on surface the ductility of the steel is reduced significantly and the material is in brittle stage. Figure 2.4.2 shows a picture of one of the tested tensile specimen revealing severe cracking during testing due to hydrogen uptake and cracking. In these cases, the material is unable to react to higher tensile stress such as due to cooling and warming up again. The experience from operating wells in these fields have not showed any incidents like cracking of the well casing materials so the stresses are probably lower than the brittle material can tolerate. This is though a concern if the need for rapid cooling occurs.

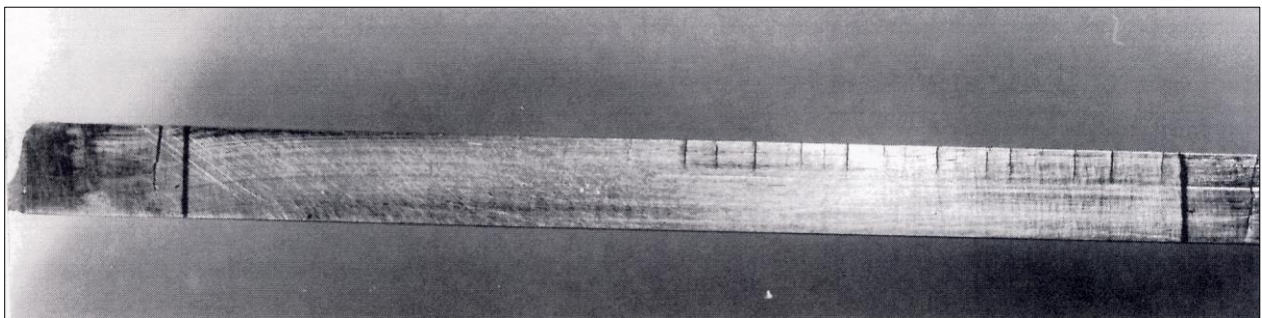


**Figure 2.4.2.** A tensile testing specimen after slow stain testing. Material taken from Well NJ 5 in the Nesjavellir geothermal area in Iceland. Several cracks formed during testing revealing hydrogen embrittlement. (Thorbjornsson, 1994).

In Figure 2.4.3 two specimens from tensile testing of material from the KJ – 39 well in Krafla are shown. It can clearly be seen that the specimen taken from liner section 53 has a brittle fracture but the one from first section of the liner is with ductile fracture. This is due to Hydrogen Embrittlement as discussed earlier and revealed in Figure 2.2.

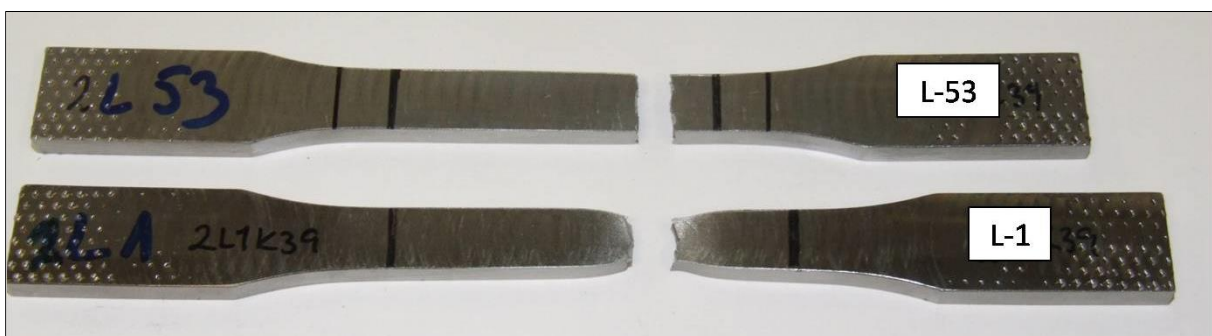


**Figure 2.4.3.** A tensile testing specimens after slow stain testing. Material taken from liner, L-1 is from the first section of the liner and L-53 from the 53rd section of the liner. L-1 is with ductile fracture but the specimen from L-53 with brittle fracture. (Karlsdottir and Thorbjornsson, 2013).

## 2.5 Stress corrosion cracking

Stress corrosion cracking (SCC) is a phenomena were stress, material composition and environmental effects play a vital role. SCC is often connected to, but not only, use of stainless steels of the austenitic type. When tested in geothermal the use of pre stressed specimen is used. In following the discussion will be on so called U-bend specimens with two strain levels, 12.5 and 20% and the testing was done in the IDDP-1 well in Krafla geothermal area (Karlsdottir et al., 2015). No cracking was found in the S235 carbon steel as expected. SCC cracks are observed in the S30403 and S31603 austenitic stainless steels at both strain levels, and for the S31803 duplex stainless steel at the higher strain level. The cracks that are identified as SCC cracks are cracks that are perpendicular to the surface and the tensile stress as is conventional for SCC cracks. Different kinds of damages, crack-like, were found in cross-sections of the N08904, S312542, and S32750 U-bend specimens at the higher strain level and for the S31803 specimen at the lower strain level. These cracks are parallel to the metal surface, as can be seen in Figure 2.5.2, 2.5.3 and 2.5.4, and thus cannot be attributed directly to SCC; indicating at least a different cracking mechanism to that of the conventional stainless steel. The S30403, S31603 and S31803 all have lower molybdenum (Mo) content between 0-3.5% while the other stainless steels have higher than 4% Mo. Mo is known to increase the resistance to pitting and crevice corrosion in stainless steels but it is not evident here whether that influenced the SCC crack formation.



**Figure 2.5.1.** *Stress corrosion cracking on the outside of a pipe from AISI 316 stainless steel (Photo Thorbjornsson).*

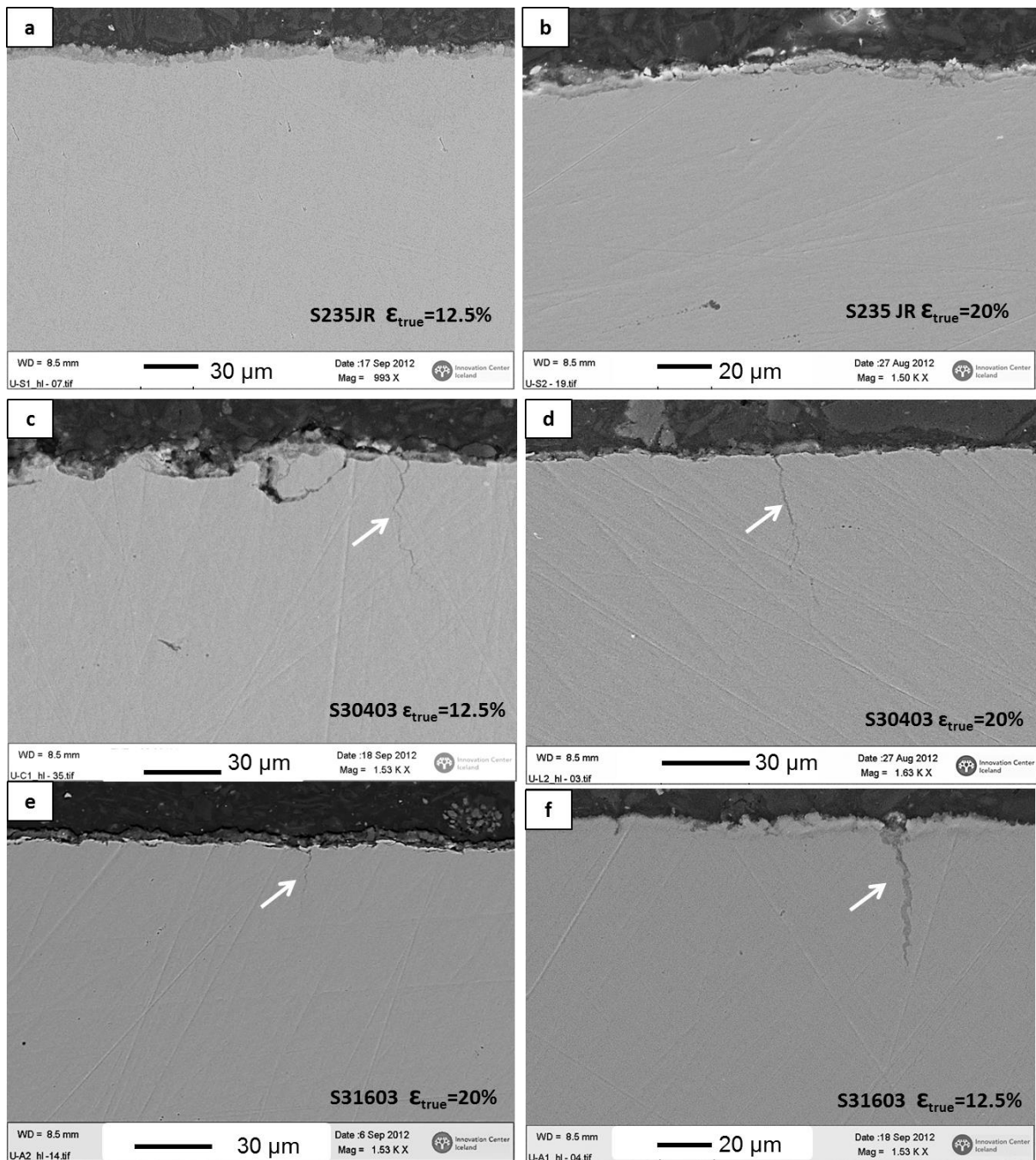


**Figure 2.5.2.** SEM images of the cross-section of the U-bend specimens; (a)-(b) the carbon steel with no SCC cracks; and (c)-(f) the S30403 and S31603 austenitic stainless steels with SCC (Karlsdottir et al., 2015).

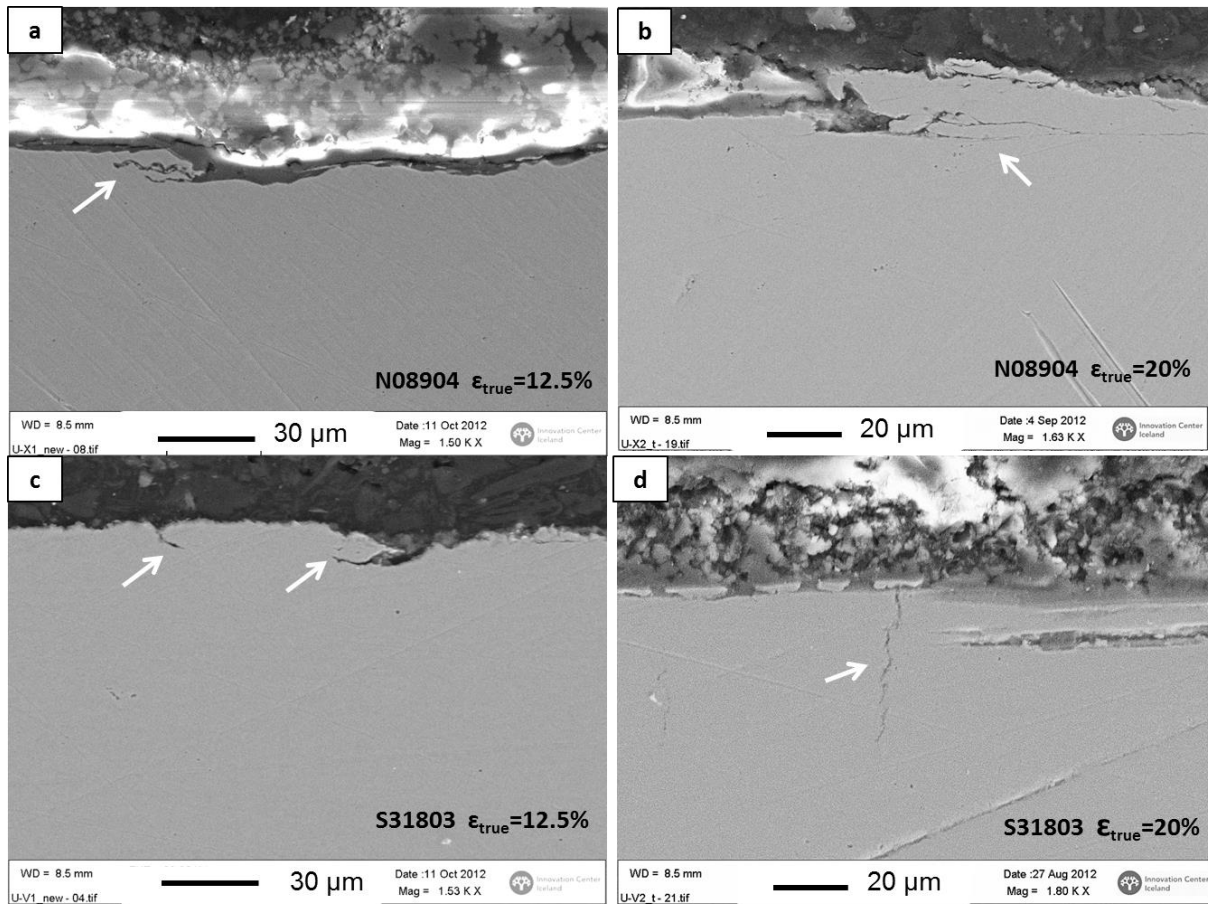


**Figure 2.5.3.** SEM images of the cross-section of the U-bend specimens; (a)-(b) the N08904 with parallel crack like damages at both strain levels; (c)-(d) the S31803 duplex stainless steels with parallel crack like damages at lower strain level and SCC cracks at the higher strain levels. (Karlsdottir et al, 2015).

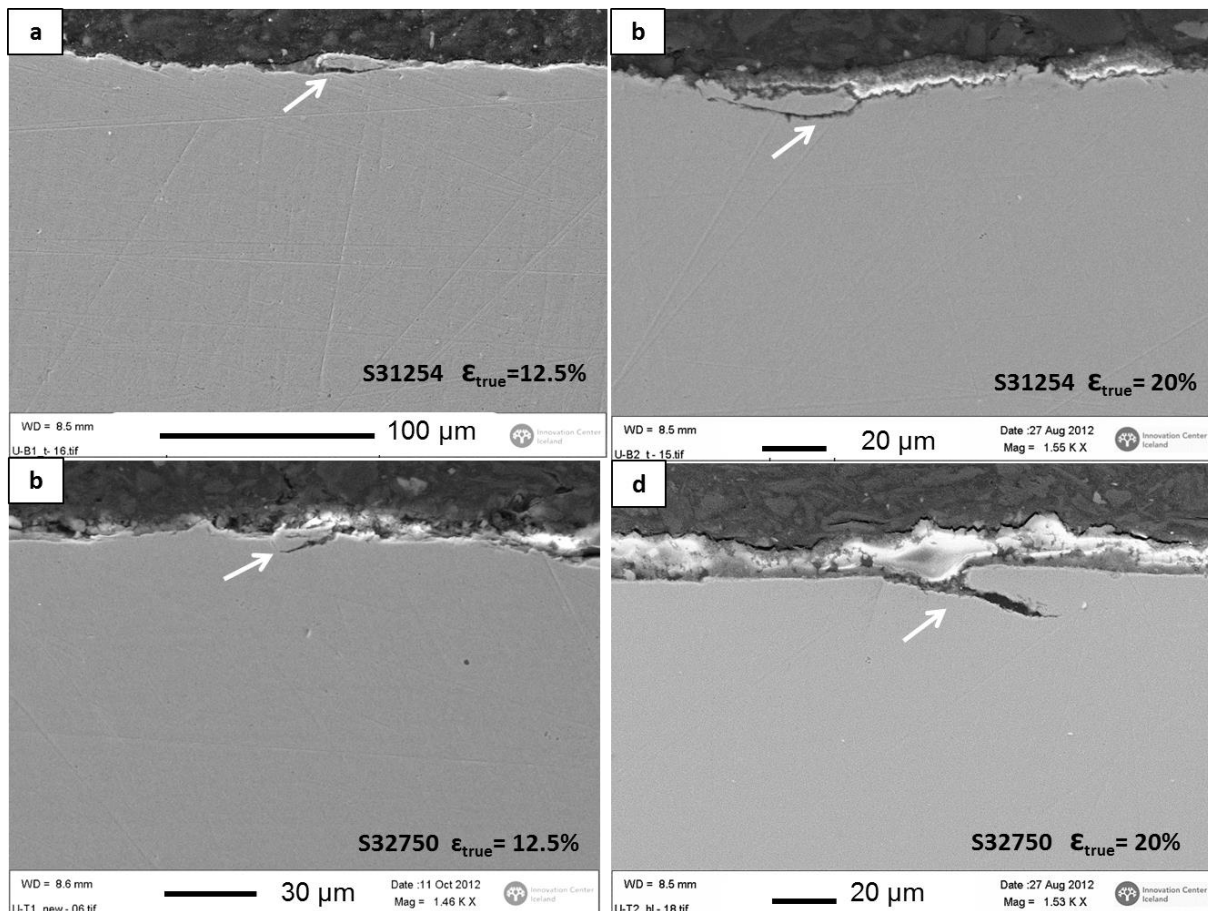


**Figure 2.5.4.** SEM images of the cross-section of the U-bend specimens; (a)-(b) the S31254 austenitic stainless steel and (c)-(d) the S32750 duplex stainless steels with parallel crack like damages at both strain levels. (Karlsdottir et al., 2015).

## 2.6 Galvanic corrosion

Galvanic corrosion is due to metallic connection between two metals of different types or chemical composition with electrolyte on the surface. Metals have different steady-state electrode potential according to their composition and this can be seen in the galvanic series for metals in sea water as shown in figure 2.6.1

Connecting two alloys in electrolyte, such as water, can lead to anode-cathode reaction where the less noble metal will dissolve to give electrons to protect the more noble alloy. This can clearly be seen in figure 2.6.2 where one-way valve from cold water well for cooling water made from cast iron house has a bronze connector and sieve. The cast Iron as less noble than the bronze is suffering from rapid corrosion.

Material	Steady-state electrode potential, V versus SCE
Graphite . . . . .	+0.25
Platinum . . . . .	+0.15
Zirconium . . . . .	-0.04
AISI type 316 stainless steel (passive) . . . . .	-0.05
AISI type 304 stainless steel (passive) . . . . .	-0.08
Monel alloy 400 . . . . .	-0.08
Hastelloy alloy C . . . . .	-0.08
Titanium . . . . .	-0.10
Silver . . . . .	-0.13
AISI type 410 stainless steel (passive) . . . . .	-0.15
AISI type 316 stainless steel (active) . . . . .	-0.18
Nickel . . . . .	-0.20
AISI type 430 stainless steel (passive) . . . . .	-0.22
Copper alloy C71500 (70Cu-30Ni) . . . . .	-0.25
Copper alloy C70600 (90Cu-10Ni) . . . . .	-0.28
Copper alloy 442 (admiralty brass)(a) . . . . .	-0.29
G bronze . . . . .	-0.31
Copper alloy . . . . .	-0.32
Copper . . . . .	-0.36
Copper alloy C46400 (uninhibited naval brass) . . . . .	-0.40
AISI type 410 stainless steel (active) . . . . .	-0.52
AISI type 304 stainless steel (active) . . . . .	-0.53
AISI type 430 stainless steel (active) . . . . .	-0.57
Carbon steel . . . . .	-0.61
Cast iron . . . . .	-0.61
Aluminum alloy 3003-H . . . . .	-0.79
Zinc . . . . .	-1.03

**Figure 2.6.1.** *The galvanic series in sea water. More noble alloys on the top (corrosion resistant) and more reactive as the potential decrease.*



**Figure 2.6.2.** *Figure showing severe galvanic corrosion on one-way valve where the house is made of Cast Iron with connector and sieve made of Bronze. (Photo by A. Einarsson).*

### 3 Materials for geothermal wells

Materials for geothermal wells have mainly been from carbon steels were the wells casings and liners are from API types, such as J55, K55, L80 and T95 steels. In recent years and specially to cope with very sour wells the use of Titanium casings (Salton Sea USA) and cladding like in IDDP-1 were the expansion spool was weld cladded with 309 type stainless steels. Research for better corrosion resistant materials have been performed as described in section 2 of this report and in the following sections each material type will be discussed.

#### 3.1 Carbon steels

Carbon steels or low alloy steels with less than 0.25% C and 0.4-1.5% Mn are the dominating materials used for geothermal wells, for pipes and equipment above ground. In general, this material has shown to be both economic and long lasting for the geothermal wells mainly used in Icelandic high temperature wells is API K55 grade. API TN95 has been used were higher strength and creep resistance is required like in the uppermost section of the IDDP-1 well. In general carbon steel has shown long lasting properties in geothermal use, but with the exception were the pH level has dropped and when condition has allowed condensation on the material surface, see chapter 2. This is also the experience from the corrosion testing experiment where the carbon steel specimens in direct contact to the superheated IDDP-1 steam at 360°C measured with corrosion rates below 0.1 mm/year. The low amount of additives in the TN95 does not help in corrosion resistance and the pitting corrosion was actually quite extensive for the TN95 in the IDDP-1 steam testing (Karlsdottir et al., 2014). Above ground in diverse equipment the carbon steels have suffered from erosion-corrosion problems as can be seen from the erosion-corrosion test with the IDDP-1 steam (Karlsdottir et al, 2014). However, carbon steels are good candidates for use in controlled conditions where condensate can be avoided and where erosion-corrosion is not a problem.

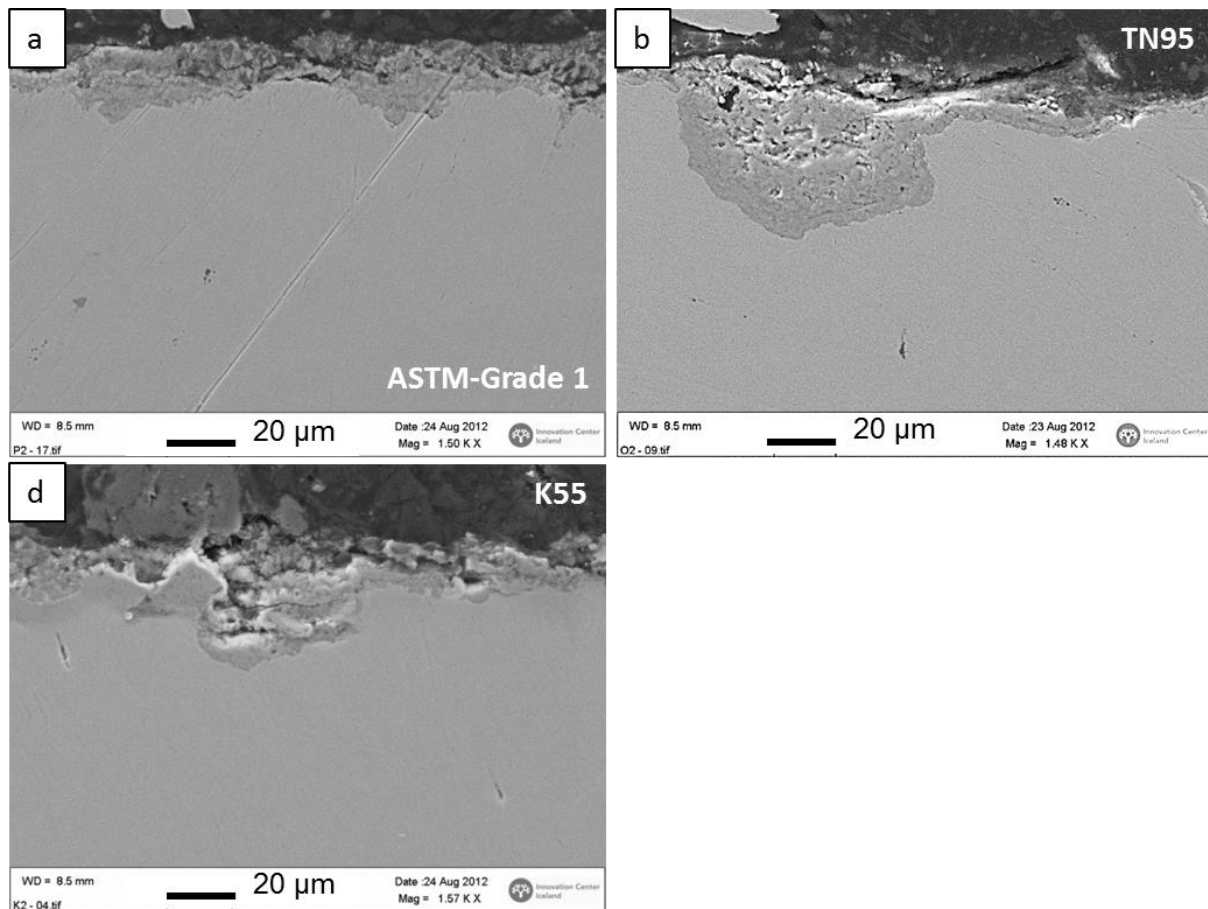


**Figure 3.1.1.** SEM images of the cross-sections of the carbon steels after testing (a) ASTM Grade A-1, (b) API TN95, and (c) API K55 (Karlsdottir et al., 2015).

### 3.2 Stainless steels

Stainless steels are steels containing more than 12% Cr and are often alloyed further with Ni, Mo and N. Stainless steels have a wide use in applications in the geothermal power production, mainly in diverse equipment's and piping. They have not been used in geothermal wells in Iceland. In general, this material group can be divided into two major groups when used in geothermal fields, Austenitic stainless steels and Duplex stainless steels. Both groups have long history of use in geothermal fields in Iceland and have been proven as a proper material for wide variety of applications. For higher temperatures above 250°C it is not recommended to use the Duplex type due to its structural change, shown as change in the material tensile strength above that temperature. Testing in IDDP-1 steam has shown erosion-corrosion damage for S32707 (Karlsdottir et al., 2014). Below 250°C the Duplex types S32507 and S32707 have both excellent resistances to corrosion and during testing in IDDP-1 practically no problems in use were detected. The Austenitic types can in fact be divided into two types, the lower alloyed types AISI 304 and AISI 316 and then the higher alloyed S31254, N08904 and N08028. The 304/316 types have shown to have limited resistance to corrosion and suffer from diverse corrosion forms in high temperature steam such as in IDDP-1. These results indicate limited use for these lower alloyed austenitic stainless steels in such conditions. The higher alloyed austenitic steels have shown better performance, especially the S31254 type. In one instance, the heat exchanger test, evidence of intergranular stress corrosion cracking was found in this material which was the only case where problems were found with the

S31254 material (Karlsdottir et al, 2014). In general, the stainless steels, especially the higher austenitic grades, can be considered as good candidate materials for use in high temperature geothermal steam with temperatures above 250°C.

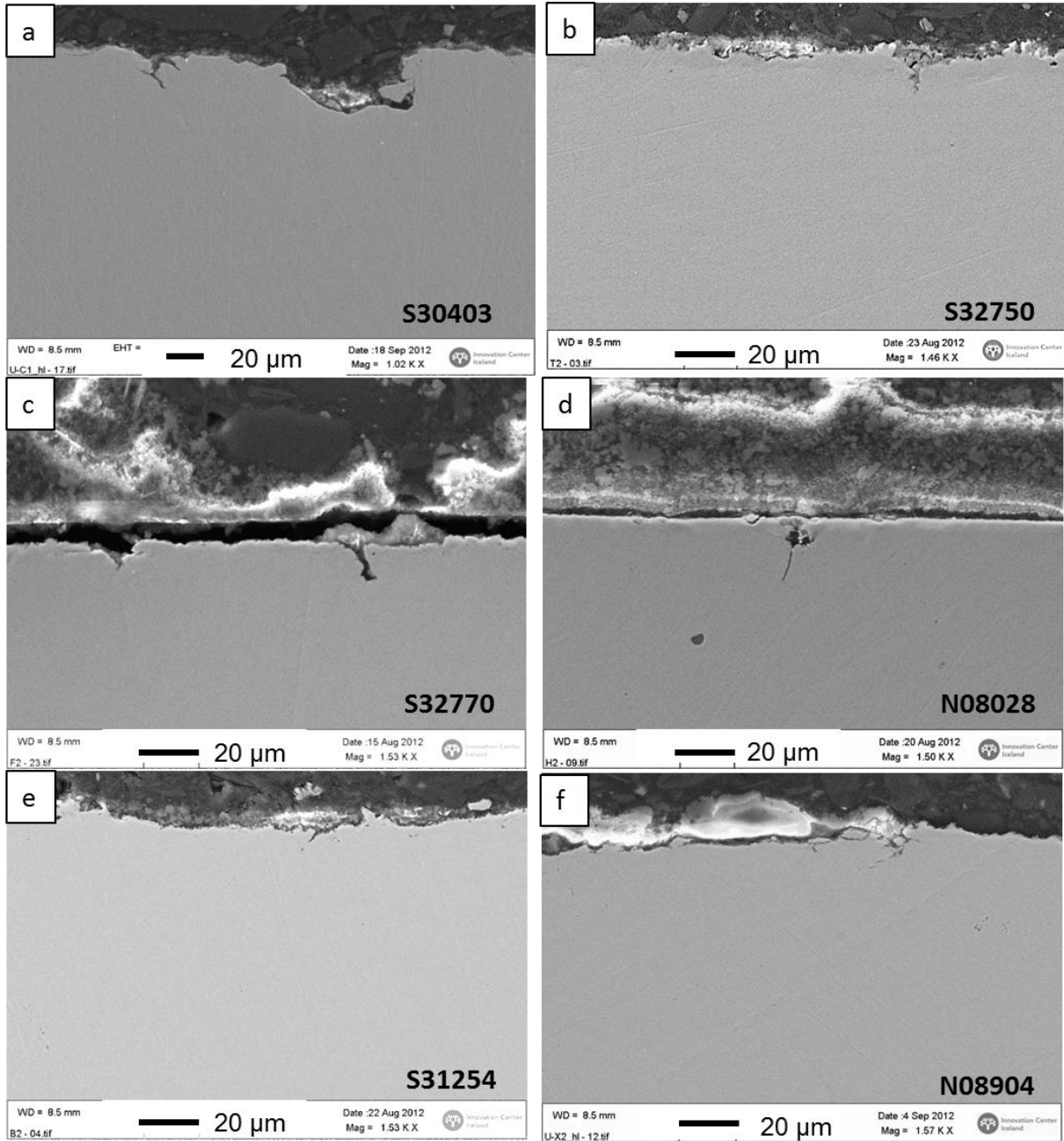


**Figure 3.2.1.** SEM images of the cross-sections of the stainless steels after testing (a) S30403, (b) S32750, (c) S32770, (d) N08028, (e) S31254 and (f) N08904. (Karlsdottir et al., 2015).

### 3.3 Nickel alloys

Nickel based alloys with Nickel content below 60% have long tradition for being good materials for diverse harsh environments such as geothermal environment. These alloys have not been widely used in geothermal steam in Iceland so limited practical experience has been obtained. Testing in IDDP-1 high temperature geothermal steam where N08825 and N06625 nickel alloys were tested revealed that even these corrosion resistant materials have some concerns in use. The N08825 type suffered from corrosion pitting after testing in the IDDP-1 steam and even the higher alloyed N06625 type showed evidence of small corrosion damage in the form of narrow pitting in the heat exchanger test, the corrosion testing in the IDDP-1 steam at 360°C and in the wet scrubbing experiments. Further testing of these materials is needed for better clarification of their use in high temperature geothermal steam.

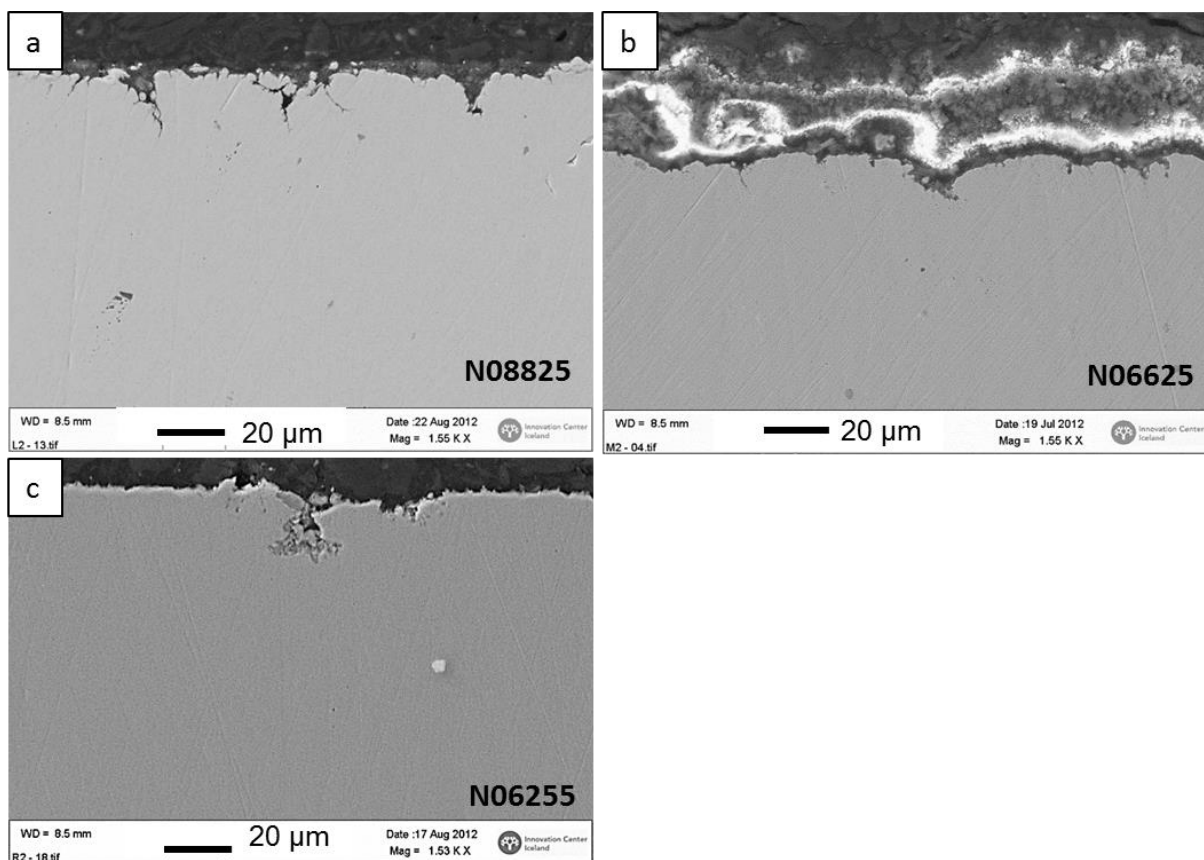


**Figure 3.3.1.** SEM images of the cross-sections of the nickel alloys after testing (a) N08825, (b) N06625, and (c) N06255. (Karlsdottir et al., 2015).

### 3.4 Titanium

Two types of titanium alloys were tested in the IDDP-1 steam, type R50400 and R52400. The R50400 type suffered from narrow pitting but the R52400 type alloyed with Pd showed more resistance. There is some concern with regard to HF containing steam like in IDDP-1 for the R50400 type were the R50400 has more resistance to HF containing steam due to the Pd alloying. In general, the concern of strength for Titanium alloys can limit their use at higher temperatures (>400°C). The possibility of hydrogen embrittlement is also of concern for low pH environment at higher temperatures (>80°C).

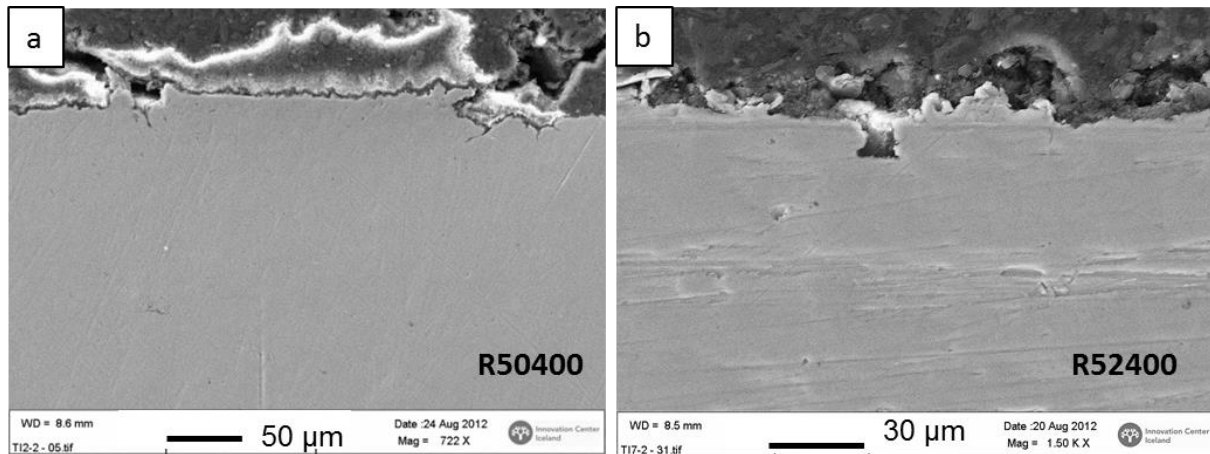


**Figure 3.4.1.** SEM images of the cross-sections of the titanium alloys after testing (a) R50400, and (b) R52400. (Karlsdottir et al., 2105).

## 4 Conclusions

This report describes a series of material testing in several high temperature wells, both as a research results and as a failure analyses. Main focus has been on the Iceland Deep Drilling experience, no well has been drilled were the temperature is higher and more material research conducted on a single well. The energy from IDDP-1 was calculated to be sufficient for up to 35 MWe where the mean energy from high temperature wells are close to 7.5 MWe in Iceland (Sveinbjornsson and Thorhallsson, 2013). Materials tested in the IDDP-1 steam were of four types, low alloy carbon steels, Stainless steels, Nickel based alloys and Titanium alloys. Not all of the steel types were tested in all test setups, relevant material types were selected for each setup. Based on the findings from testing in the IDDP-1 steam together with findings the authors have got from other high temperature geothermal wells, the following remarks regarding material selection can be made: (Thorbjornsson et al, 2015)

**Carbon Steel.** Carbon steels or low alloy steels are the dominating material used for geothermal wells, for pipes and equipment above ground. In general, this material has shown to be both economic and long lasting for the geothermal wells. API K55 grade is mainly used and API L80 for connectors. API TN95 has been used were higher strength and creep resistance is required such as for the uppermost section of the safety casing in IDDP-1. In general carbon steel has shown long lasting properties in geothermal use, but with the exception were the pH level has dropped and when the conditions have allowed condensate on the material surface. This is also the experience from the corrosion testing experiment where the carbon steel specimens in direct contact to the superheated IDDP-1 steam at 360°C showed corrosion rates below 0.1 mm/year. The low amount of additives in the TN95 does not help in corrosion resistance and the pitting corrosion was actually quite extensive for the TN95 in the IDDP-1 steam testing (Karlsdottir et al., 2014). Above ground in diverse equipment the carbon steels have suffered from erosion-corrosion problems as can be seen from the erosion-corrosion test with the IDDP-1 steam (Karlsdottir et al, 2014). However, carbon steels are good candidate for use in controlled conditions where condensate can be avoided and where erosion-corrosion is not a problem. Within the GeoWell project it is proposed that the K55, L80 and TN95 will be further tested as well as High Strength – High Sulphur resistant materials.

**Stainless Steels.** Stainless steels have a wide use in geothermal power production, mainly in diverse equipments and piping. They have not been used in geothermal wells in Iceland. In general, this material group can be divided into two major groups when used in geothermal fields, Austenitic stainless steels and Duplex stainless steels. Both groups have long history of use in geothermal fields in Iceland and have been proven as a proper material for wide variety of applications. For higher temperatures above 250°C it is not recommended to use the Duplex type due to its structural change, shown as change in the material tensile strength above that temperature. Testing in IDDP-1 steam has shown erosion-corrosion damage for S32707 (Karlsdottir et al., 2014). Below 250°C the Duplex types S32507 and S32707 have both excellent resistances to corrosion and during testing in IDDP-1 practically no problems in use were detected. The Austenitic types can in fact be divided into two types, the lower alloyed types AISI 304 and AISI 316 and then the higher alloyed S31254, N08904 and N08028. The 304/316 types have shown to have limited resistance to corrosion and suffer from diverse corrosion forms in high temperature steam such as in IDDP-1. These results indicate limited use for these lower alloyed austenitic stainless steels in such conditions. The higher alloyed austenitic steels have shown better performance, especially the S31254 type. In one instance, the heat exchanger test, evidence of intergranular stress corrosion cracking was found (Karlsdottir et al., 2014) in this material which was the only case where problems were found with the S31254 material. In general, the stainless steels, especially the higher austenitic grades, can be considered as good candidates materials for use in high temperature geothermal steam with temperatures above 250°C. Within the GeoWell project it is proposed to include AISI 316 as a reference type, S31254, N08904 and N0828 for the higher alloyed austenitic steels and for duplex to continue the research on S32507 and S32707. Strong support from material providers has been very beneficial and it is proposed to seek their advice about this selection.

**Nickel based alloys.** Nickel based alloys have long tradition of being good materials for diverse harsh environments. These alloys have not been widely used in geothermal steam in Iceland so limited practical experience has been obtained. Testing in IDDP-1 high temperature geothermal steam where N08825 and N06625 nickel alloys were tested revealed that even these corrosion resistant materials have some concerns in use. The N08825 type suffered from corrosion pitting after testing in the IDDP-1 steam and even the higher alloyed N06625 type showed evidence of small corrosion damage in the form of narrow pitting in the heat exchanger test, the corrosion testing in the IDDP-1 steam at 360°C and in the wet scrubbing experiments. Further testing of these materials within GeoWell is needed for better clarification of their use in high temperature geothermal steam.

**Titanium alloys.** Two types of titanium alloys were tested in the IDDP-1 steam, type R50400 and R52400. The R50400 type suffered from narrow pitting but the R52400 type alloyed with Pd showed more resistance. There is some concern with regard to HF containing steam like in IDDP-1 for the R50400 type were the R50400 has more resistance to HF containing steam due to the Pd alloying. In general, the concern of strength for Titanium alloys can limit their use at higher temperatures (>400°C). The possibility of hydrogen embrittlement is also of concern for low pH environment at higher temperatures (>80°C). In GeoWell the grade R56320 (ASTM grade 9) will be added both as a “stand alone” material and if possible as clad material.

The material testing in the IDDP-1 pilot testing has been reviewed and the main results reported and discussed to evaluate the possibilities of utilizing superheated steam from a deep high temperature/pressure geothermal well (IDDP-1). The main results are that the corrosion rate in the IDDP-1 superheated steam where silica scaling is present is below 0.1 mm/year, which are good news.

On the down side the results from the tests indicate that the superheated steam nevertheless promotes localized corrosion in some extent in all the materials tested ranging from carbon steel, stainless steels to nickel based and titanium alloys. Of the materials tested the N06625 based nickel alloy and the R52400 titanium alloy seem to be the least effected by corrosion. The austenitic stainless steel S31254 is a promising candidate material and performs well in the majority of the tests except in the heat exchanger experiment where intergranular SCC was observed.

## 5 References

- Hauksson, T., Markusson, S.H., Einarsson, K., Karlsdóttir, S.N., Einarsson, A., Möller, A. and Sigmarsson, T. (2014). Pilot testing of handling the fluids from the IDDP-1 exploratory geothermal well, Krafla, N.E. Iceland. *Geothermics* 49, 76–82.
- Karlsdottir, S.N. and Thorbjornsson, I. (2012). Hydrogen Embrittlement and Corrosion in High Temperature Geothermal Well. *NACE International, Corrosion 2012*.
- Karlsdottir, S.N. and Thorbjornsson, I. (2013). Corrosion Testing Down-Hole in Sour High Temperature Geothermal Well in Iceland. *NACE International Corrosion 2013, paper no. 2550*.
- Karlsdottir, S.N., Ragnarsdottir, K.R., Thorbjornsson, I.O. and Einarsson, A. (2015). Corrosion testing in superheated geothermal steam in Iceland. *Geothermics Jan 2015*.
- Sveinbjornsson, B.M. and Thorhallsson, S. (2013). Drilling performance and productivity of geothermal wells – Case history from Hengill Geothermal Area in Iceland. *American Rock Mechanics Association. 47<sup>th</sup> US Rock Mechanics/Geomechanics Symposium San Francisco USA June 2013*.
- Thorbjornsson, I. (1995). Corrosion fatigue testing of eight different steels in an Icelandic geothermal environment. *Materials & Design Volume 16 1995*.
- Karlsdottir, S.N., Ragnarsdottir, K.R., Moller, A., Thorbjornsson, I.O., Einarsson, A. (2014). On-Site erosion-corrosion testing in superheated geothermal steam. *Geothermics* 51 p 170-181.
- Thorbjornsson, I.O., Karlsdottir, S.N., Einarsson, A. and Ragnarsdottir, K.R. (2015). Materials for Geothermal Steam Utilization at Higher Temperatures and Pressure. *Proceedings World Geothermal Congress, Melbourne Australia. 2015*.
- Thorbjornsson, I.O. (1994) Samples retrieved from well nr. 8 in Reykjanes. Unpublished work for HS-ORKA. In Icelandic.
- Karlsdottir, S.N., Thorbjornsson, I.O., Ragnarsdottir, K.R., and Einarsson, A. (2014). Corrosion testing of heat exchanger tubes in steam from the IDDP-1 exploratory geothermal well in Krafla, Iceland. *NACE International conference, Corrosion 2014*.